Moscow University
Physics Bulletin
Vol. 53, No. 4, pp. 79–83, 1998

Vestnik Moskovskogo
Universiteta. Fizika
UDC 537.52.77; 502.614.7

PHYSICAL FOUNDATIONS FOR RADIOMETRIC MONITORING OF ATMOSPHERIC MINOR GAS COMPONENTS

Sh. D. Kitai, A. P. Naumov, and N. N. Osharina

Rotational spectrum data are presented for minor gas components which possess dipole moments. A set of components was established that can be diagnosed in the low and medium atmosphere by microwave radiometry techniques in observations from the Earth surface and from satellites, including limb sensing.

The in-principle feasibility of the radiometric monitoring of minor gas components (MGC) in the atmosphere is based on the properties of the inherent (thermal) radio emission, generated by atmospheric gases that have magnetic or electric dipole moments. These gases have emission/absorption maxima at their molecules' resonance frequencies. Measuring the level of atmospheric thermal emission near MGC resonances, one can obtain information on the content of pollutive gas components. The frequencies of rotational spectra of gas molecules are located in the radio band. For this reason, in radiometric monitoring one deals with simpler atmospheric gas spectra than in the IR and visual bands, in which vibrational and electron quantum transitions are respectively located. Table 1 gives a list of some atmospheric gaseous impurities whose molecules possess dipole moments and can, in principle, be detected by their inherent thermal radio emission.

The rotational spectra of MGCs have the following features: the broadening of absorption lines and bands is caused by binary molecular collisions at altitudes from the Earth surface of up to about 60 km. These collisions are diabatic, i.e., they are accompanied by permitted quantum transitions, in contrast to adiabatic collisions in the IR and optical spectral bands. Molecular collisions also determine the overall shape of the spectral lines located in the microwave band. It is well known that the formation of a line's central portion (with small frequency deviations from the resonance $\Delta\omega$) results from the collisions of far-flying molecules: $\Delta\omega \sim r^{-m}$, where r is the impact parameter. Such collisions are quite accurately described by the kinetic theory. As a result, the impact theory, which is valid when $\tau_c^{\text{eff}} \ll 1/\Delta\omega$, quite adequately describes the characteristics of microwave energy absorption and emission in the resonance spectrum regions. In the above inequality, τ_c^{eff} is the effective duration of molecule collisions, equal to the ratio of the collision time to the number of quantum transitions in that period. A fundamental reason for the feasibility of MGC radiometric monitoring is the fact that many spectral lines and bands of impurities lie in the atmosphere's transparency windows. This makes it possible to isolate the MGC contributions by their spectral features against the background of absorption and emission by the primary molecular components of the atmosphere (water vapor and oxygen), providing for reliable quantitative interpretation of the data produced by radiometric measurements in impurity resonance regions.

These facts characterize the advantages inherent in radiometric MGC monitoring. However, there are some difficulties. First, diagnosing MGCs by their radio emission in the microwave band is a difficult task of isolating weak signals against the background of the atmosphere's strong emission. Secondly, in overlapping absorption bands, the intensity of the pure atmosphere self-emission (i.e., the background) becomes a nonlinear function of frequency, which must be correctly accounted for. Furthermore, calculations of the

Radiophysical Research Institute, Nizhnii Novgorod.

Table 1

MGC Dipole Moments and Radio Brightness Contrasts ΔT_b in Impurity Resonance Regions for the Pollution Layers 100–200 m (ΔT_{b1}) and 0–500 m (ΔT_{b2})

Gas	μ_i, D	ν, GHz	ΔT_{b1}, K	ΔT_{b2}, K
CO	0.112	115.3	<0.1	<0.1
		230.5	<0.1	0.1
COS	0.709	146.0	0.6	2.8
		279.7	1.0	5.0
HNO_3	2.0	143.7	2.4	11.6
		294.3	4.6	19.2
HCN	2.984	88.6	2.6	12.5
		265.9	10.3	38.7
HOCl	1.471	98.1	0.3	1.5
		291.3	0.6	2.6
H_2CO	2.31	140.8	0.9	4.6
		291.4	3.2	14.1
H_2O_2	1.573	91.4	0.6	3.0
		251.9	0.5	2.5
H_2S	1.02	168.9	0.2	1.1
NH_3	1.468	24.0	0.9	4.2
NO	0.16	150.5	<0.1	0.1
		250.5	<0.1	0.2
NO_2	0.29	98.0	<0.1	0.1
		156.2	<0.1	0.1
		277.9	0.1	0.4
N_2O	0.166	150.7	<0.1	0.1
		276.3	0.1	0.3
SO_2	1.634	130.9	1.1	5.5
		282.3	1.9	8.7
ClO	1.2974	130.0	0.9	4.5
		278.6	2.7	12.1

atmospheric radio emission in overlapping MGC bands (computation of integral equation kernels for solving remote sensing inverse problems) must be carried out with due regard for spectral line interference, but the quantitative theory of such effects has not yet been elaborated in sufficient detail. The main reason is the lack of necessary spectroscopic measurements, rather than any difficulties with the basic techniques. Finally, there are technical problems in designing wideband ($\delta\nu \cong 5$–10 GHz) microwave radiometer channels for spectral analysis of the emission bands in question. Some of these difficulties can be surmounted with the aid of the measurement techniques developed for the purposes of radio astronomy (see, e.g., [1]), other problems still remain to be solved.

In this paper we discuss the possibilities of MGC detection in the lower atmospheric layers by remote sensing from the Earth surface and in the middle atmosphere by remote sensing from a satellite using the limb geometry. The capabilities of radiophysical MGC detection techniques are analyzed using the

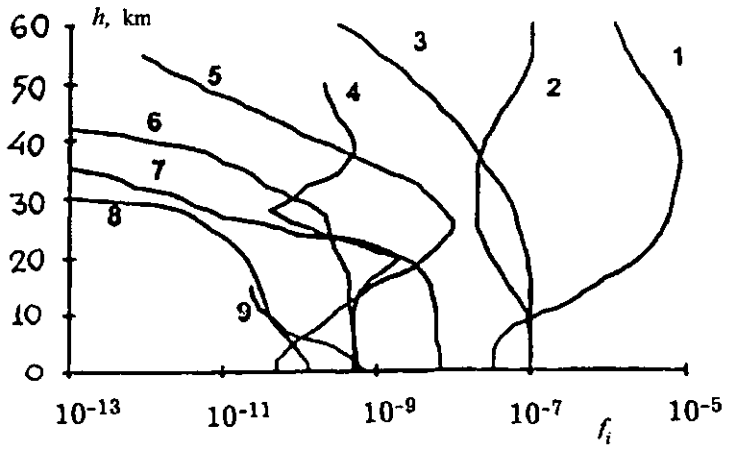

Fig. 1

Altitude distributions of background relative concentrations of some MGCs: (*1*) O_3, (*2*) CO, (*3*) N_2O, (*4*) ClO, (*5*) HNO_3, (*6*) COS, (*7*) NH_3, (*8*) SO_2, (*9*) H_2CO.

altitude profiles of impurity component background concentrations f_i (Fig. 1), information on their highest admissible concentrations (HAC), quantitative data on actual HAC violations, parameters of the millimeter-wave absorption spectra of MGCs and the primary gaseous components of the atmosphere, water vapor and oxygen, and algorithms for calculating coefficients of absorption, optical thicknesses, and the radio brightness temperatures of the atmosphere when observed from different platforms. Dealing with pollution in the lower atmospheric layers, these characteristics were analyzed for the impurities listed in Table 1. In addition to these gases, ozone was considered for evaluating the possiblity of detecting background concentrations of impurities. The spectral data were taken from the GEISA [2] and HITRAN [3] data banks.

Figure 2 shows the coefficients of absorption for seven impurity components in the centimeter and millimeter bands for the standard sea-level atmospheric conditions (pressure $P = 760$ mm Hg, temperature $T = 293$ K, absolute humidity $\rho = 7.5$ g/m^3), for the concentrations f equal to their HAC values, and the coefficient of absorption for pure atmosphere which is due to water vapor and molecular oxygen. The figure shows that the absorption by impurity gases at the Earth surface is lower than the absorption by the primary atmospheric gases, for both background and even highest admissible MGC concentrations. Calculations show that at certain altitudes H_i (different for different MGCs) the contributions from impurities and the primary atmospheric gases become equal in some resonance regions, and at higher altitudes ($h > H_i$) the MGC contributions become dominant. The values of H_i in the optimum resonance regions are: 13 km for O_3, 16 to 19 km for N_2O, HNO_3, ClO, and HOCl, and 24 to 32 km for CO, H_2O_2, and NO.

The optimization of MGC remote sensing conditions includes the determination of the operating frequencies and observation angles for which the radio brightness temperature contrasts $\Delta T_b = T_b - T_{ab}$ become measurable and assume their highest values. Here T_b is the brightness temperature of the atmosphere in the presence of the gas component to be detected, T_{ab} is the brightness temperature in the absence of that component (background temperature). Table 1 lists the values of ΔT_{ab} for remote sensing in the zenith direction, for relative MGC concentration $f = 10^{-5}$, in summer. Contrast estimates ΔT_b for other values of low concentrations f and pollution layers Δh can be obtained by linear interpolation between the table values. The pollution mixing layer usually varies in the range of about 200 to 500 m.

Modern microwave radiometers are capable of recording weak signals with radio brightness contrasts of about 0.1 K on the atmospheric background [1]. Thus, the radiometric method can be used for remote detection of ammonia, sulphurous anhydride, and sulphuretted hydrogen pollutions in industrial areas. The concentration of pollutants in exhausts may exceed HAC values, depending on the pipe height, by a factor of 10^3 to 10^6 or more. The radio brightness contrasts for natural background MGC concentrations f_i are low: $\Delta T_b \leq 0.1$–0.3 K, but they increase by several times at the optimum observation angles (especially in winter) and, of course, they become greater with increasing MGC concentrations. For ozone the contrasts

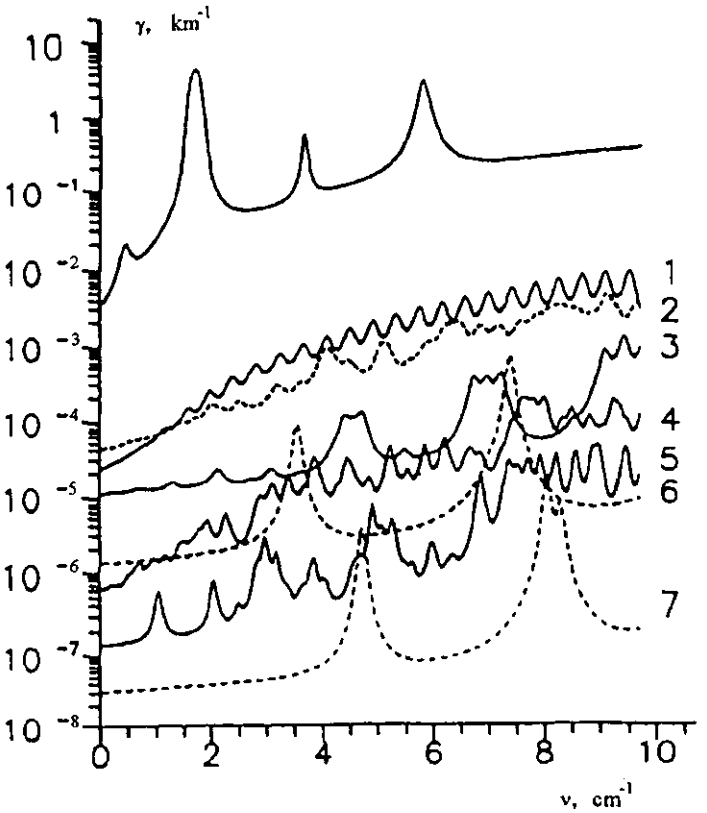

Fig. 2

Coefficients of absorption for impurity components (*1*—HNO_3, *2*—SO_2, *3*—H_2CO, *4*—O_3, *5*—NO_2, *6*—CO, *7*—NO) for standard atmospheric conditions at sea level (pressure $P =$ 760 mm Hg, temperature $T = 293$ K) and concentrations equal to HAC values. The upper curve is the summary absorption coefficient due to water vapor and molecular oxygen.

ΔT_b are about 10 K at average background concentrations, which is widely used today in radiometric O_3 monitoring.

Results of remote sensing of ammonia at $\nu \sim 25$ GHz and of sulphurous anhydride at $\nu \sim 131$ GHz in industrial exhausts were reported in [4, 5]. Attempts of microwave measurements (at $\nu \cong 115$ and 230 GHz) of carbon oxide content in the mesosphere were described in [6].

The calculated increments of radio brightness temperatures ΔT_b for the case of satellite observations in the nadir direction (over a smooth water surface) usually do not exceed fractions of a degree (about 0.1–0.3 K) for the background concentrations of the most active MGCs (ClO, N_2O, HNO_3, HOCl). Ozone is again an exception: $\Delta T_b \cong 4$–7 K at the frequencies 195.43, 237.14, and 286.16 GHz.

Very promising results in MGC content monitoring can be expected from limb remote sensing of the atmosphere. This satellite technique was described in detail in [7]. Our numerical modeling of a space experiment yielded a set of gas components (Table 2) whose background concentrations are detectable by the limb sensing technique. The data listed in Table 2 correspond to the receiving band $\delta\nu = 10$ MHz. This value of $\delta\nu$ is about 10% of the MGC spectral lines' half-width at the altitude $h_1 = 20$ km and about 50% at $h_2 = 30$ km. The radio brightness temperatures without the MGCs are $\cong$ 8–15 K for the target distance $h_n = h_1$ and fractions of a degree for $h_n = h_2$. Table 2 includes the maximum and minimum central frequencies of the millimeter-band sensing channels for which the condition $\Delta T_b(h_n) \geq 1$ K is satisfied. If the spectral resolution is enhanced to $\delta\nu = 2$ MHz, the corresponding increments of radio brightness temperatures for $h_n = 30$ km increase by a factor of 1.2–2.4. For chlorine oxide, however, the increase does not exceed 0.2 K.

Table 2

Resonance Frequencies ν_{ij}, Radio Brightness Temperature Contrasts ΔT_b at Target Altitudes 20 and 30 km, and Altitude Intervals ΔH of MGC Sensing by the Limb Technique for Background Impurity Levels

Gas	ν_{ij}, GHz	ΔT_b ($h_n = 20$ km), K	ΔT_b ($h_n = 30$ km), K	ΔH, km
CO	230.69751	4.0	8.5	15 to 42
HNO_3	294.49719	17.4	5.0	
	256.83537	17.7	4.9	15 to 50
HOCl	291.49083	9.8	2.5	
	195.63672	4.4	1.4	15 to 55
N_2O	276.51882	15.8	4.7	
	175.97736	3.6	2.4	15 to 40
ClO	278.82293	4.2	1.8	
	204.48744	2.7	1.6	15 to 35
O_3	286.356	76.1	66.2	
	142.275	65.2	38.9	15 to 75

Other gaseous components can be diagnosed at concentrations higher than the background values f_i. For instance, the increments ΔT_b ($h_n = 20$ km) for the nitrogen oxides NO and NO_2 are about 2–3 K at the resonance frequencies in the 250–293 GHz range at $f \cong (20\text{–}25)f_i$ and $\delta\nu = 10$ MHz. The corresponding values of ΔT_b for sulphide carbonyl are about 3 K in the 280–292 GHz range at $f \cong 2f_i$, and for sulphurous anhydride are about 5.5 K at 251–284 GHz and $f = 10f_i$.

It must be pointed out that the increments of radio brightness temperatures measured in [8] during satellite limb sensing of chlorine oxide at the frequency 204.387 GHz for the target altitudes $h_n \cong 20\text{–}30$ km turned out to be very close to our theoretical results, calculated with due account for the radiometer spectral parameters and sensitivities used in the experiment.

The data discussed in this paper demonstrate that radiometric MGC monitoring in the microwave band is a promising technique, which merits further research.

REFERENCES

1. N.N. Markina, A.P. Naumov, and A.V. Troitskii, *Radiotekhn. Elektron.*, vol. 40, no. 12, p. 1843, 1995.
2. A. Chedin, N. Husson, N.A. Scott, et al., *The "GEISA" Data Bank 1984 Version*, Paris, France, 1986.
3. L.S. Rothman, R.R. Gamache, A. Goldman, et al., *Appl. Opt.*, vol. 26, no. 19, p. 4058, 1987.
4. I.A. Strukov and A.V. Troitskii, *Izv. Vuzov, Radiofizika*, vol. 40, no. 6, p. 702, 1997.
5. A.P. Naumov, V.M. Plechkov, V.P. Borin, et al., *Izv. Vuzov, Radiofizika*, vol. 23, no. 5, p. 632, 1980.
6. K.F. Kunzi and E.R. Carlson, *J. Geophys. Res.*, vol. 87, no. C9, p. 7235, 1982.
7. K.P. Gaikovich, Sh.D. Kitai, and A.P. Naumov, *Issled. Zemli iz Kosmosa*, no. 3, p. 73, 1991.
8. J.W. Waters, *Proc. IEEE*, vol. 80, no. 11, p. 1679, 1992.